Dielectric Properties of Nanotube Reinforced Butyl Elastomer Composites

Thi To Nga Dang,[1,2] S. P. Mahapatra,[3] V. Sridhar,[2] J. K. Kim,[2] K-J. Kim,[2,4] H. Kwak[3]

[1]*Department of Chemical Engineering, College of Technology, Cantho University, Can Tho 92000, Vietnam*
[2]*Elastomer Laboratory, School of Nano and Advanced Materials, Gyeongsang National University, Jinju, Korea*
[3]*Department of Mechanical Engineering, Chung-Ang University, Seoul 156-756, Korea*
[4]*Department of Polymer Engineering, The University of Akron, Akron, OH*

Received 13 March 2008; accepted 9 June 2008
DOI 10.1002/app.30166
Published online 17 April 2009 in Wiley InterScience (www.interscience.wiley.com).

ABSTRACT: Dielectric relaxation behavior of multiwalled carbon nanotube reinforced butyl rubber composites has been studied as a function of variation in filler in the frequency range of 20–2 × 106 Hz. The effect of variation in filler loadings on the complex and real parts of impedance was distinctly visible, which has been explained on the basis of interfacial polarization of fillers in a heterogeneous medium and relaxation dynamics of polymer chains in the vicinity of fillers. The electric modulus formalism has been used to further investigate the conductivity and relaxation phenomenon. The frequency dependence of AC conductivity has been investigated by using Percolation theory. The phenomenon of percolation in the composites has been discussed based on the measured changes in electric conductivity and morphology of composites at different concentrations of the filler. The percolation threshold as studied by AC conductivity occurred in the vicinity of 6–8 phr of filler loading. Scanning electron microscope microphotographs showed agglomeration of the filler above this concentration and formation of a continuous network structure. © 2009 Wiley Periodicals, Inc. J Appl Polym Sci 113: 1690–1700, 2009

Key words: elastomers; nanocomposites; dielectric relaxation; percolation

INTRODUCTION

Elastomeric composites are widely used because of their light weight, design flexibility, and processability. However, these composites exhibit less attractive mechanical properties such as low strength and low-elastic modulus when compared with metals and ceramics. Adding micron or nanosized inorganic filler particles to reinforce the polymeric materials has been standard practice in the composite industry for decades.

The term filler in rubber technology is often misleading, implying a material that is primarily intended to reduce the cost of the more costly rubber. But the modern day fillers change one or more of these properties: optical properties and color, improve surface characteristics and dimensional stability, change thermal, magnetic and electrical properties, improve mechanical properties, durability, and rheology, affect chemical reactivity, biodegradability, etc. The mechanical and physical properties of the composite are mostly dominated by the nature of the filler, whereas the polymer matrix determines the environmental characteristics of the composite. Therefore, the overall composite properties can be tailored to fit the desired application through proper choice of filler and matrix resin. Therefore, a judicious choice of type of the filler and its concentration in the composite will augment the overall performance of the composite.[1]

Carbon blacks and silica have been traditionally used as reinforcing materials in elastomers. But in recent years much attention is being focused on the applicability of nanosized fillers like nanoclays,[2] exfoliated graphite,[3] carbon nanotubes.[4–6] Of these, nanotubes are being extensively investigated because besides imparting outstanding mechanical properties, nanotubes also impart distinctive conductivity, which can be used in applications that involve light weight and flexible conductive or semiconductive polymeric composites. Studies have shown that in these nanocomposites carbon nanotubes exhibit the electrical capability of acting as metallic-like conductors or having characteristics of a semiconductor depending on the chirality of the graphite lattice.[7] Compared with traditional materials, conductive nanocomposites have several advantages including extra-low threshold of particle content, no

Correspondence to: H. Kwak (kwakhy@cau.ac.kr).
Contract grant sponsor: BK21 Programme in South Korea.
Contract grant sponsor: Korean Science and Engineering Foundation; contract grant number: R01-2006-000-10358.

degradation of mechanical properties, light weight, flexibility, ability to absorb impact energy and magnetic interference, corrosion resistance, and tunable conductivity.[8]

Although there are some studies on the applicability of carbon nanotubes as reinforcing fillers in rubbers, such as natural rubber,[9–12] styrene butadiene rubber,[13,14] silicone rubber,[15] fluoroelastomer,[4] no indepth study of their dielectric properties has been undertaken. This study reports the dielectric relaxation behavior of nanotube reinforced butyl rubber in the frequency range of 20 Hz–2 MHz as function of filler loading. The effect of variation in filler loading on dielectric characteristics like real and complex parts of impedance, dielectric permittivity and conductivity have been studied. Additionally, the data obtained were also analyzed by electric modulus formalism.

EXPERIMENTAL

Materials

Lanxess butyl 101-3 isobutylene-isoprene copolymer rubber was purchased from Lanxess, Canada. Multiwalled carbon nanotubes (MWNT) of 95% were purchased from Iljin, Korea. Before usage, the nanotubes were treated with acid mixture under ultrasonication to remove amorphous carbon and metallic impurities. A sulfur-curing system has been used in this study and the curatives are stearic acid 2, zinc oxide 5, TMTD 1.5, sulfur 2 phr.[16]

Sample preparation

The compounds were mixed in a laboratory size (225 × 100 mm) mixing mill at a friction ratio of 1 : 1.25 according to ASTM D 3182 standards while carefully controlling the temperature, nip gap, mixing time, and uniform cutting operation. The temperature range for mixing was maintained at 80°C by carefully circulating water. After mixing, the elastomer compositions were molded in an electrically heated hydraulic press to optimum cure (90% of the maximum cure) using molding conditions determined by a Monsanto rheometer R-100 oscillatory disk rheometer according to ASTM D 20845 standards.

Testing

Dielectric relaxation spectra

Dielectric relaxation spectra of the composites were obtained by Agilent E4980A Precision LCR meter in the frequency range of 20 Hz–2 MHz using aluminum foil as blocking electrodes. The dielectric characteristics have been observed as a function of frequency. Electrical conductivity (σ) has been evaluated from dielectric data.

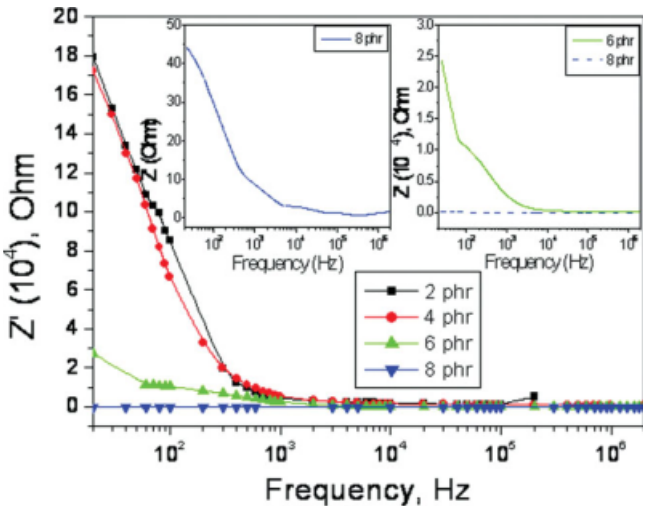

Figure 1 Effect of MWNT loadings on real part of complex impedance (Z') of butyl elastomer nanocomposites measured as a function of frequency. [Color figure can be viewed in the online issue, which is available at www.interscience.wiley.com.]

Scanning electron microscopy

Morphology of the compounds has been studied using a scanning electron microscope (SEM) [Philips XL30 S FEG(Netherlands)], after autosputter coating of the sample surface with gold.

Raman spectra

Raman spectra were recorded with a Jobin Yvon micro-Raman LabRam system in a backscattering geometry using 514.5 nm laser excitation wavelength. The laser beam was focused on the sample with the aid of an optical microscope.

RESULTS AND DISCUSSION

Complex impedance analysis

The electrical properties of butyl rubber nanocomposites filled with MWNT have been investigated using complex impedance spectroscopy (CIS). CIS is an important tool to analyze the electrical properties of the composites in view of its capability of correlating the samples' electrical behavior with its microstructure, filler loading, and dispersion.

Real part of complex impedance

Figure 1 shows variation of real part of complex impedance (Z') as a function of frequency at increasing MWNT loadings. Irrespective of the MWNT concentrations, Z' shows a monotonous decrease with

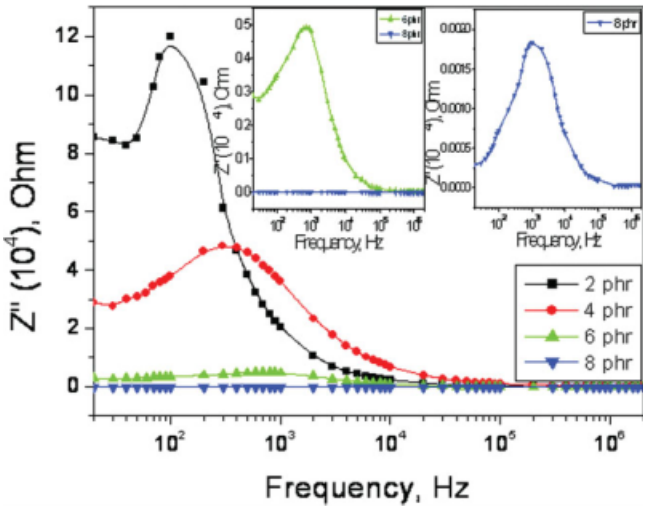

Figure 2 Effect of MWNT loadings on imaginary part of complex impedance (Z'') of butyl elastomer nanocomposites measured as a function of frequency. [Color figure can be viewed in the online issue, which is available at www.interscience.wiley.com.]

increasing frequency and curves almost merge for all MWNT loadings in the higher frequency region ($\geq 10^3$ Hz). However, in the low-frequency region, Z' value is gradually decreasing with MWNT loading. The decrease in Z' with MWNT loading and frequency indicates the possibility of increasing AC conductivity with MWNT loading and frequency (a more detailed study of AC conductivity is given in subsequent sections of the article). The merging of Z' curves in the higher frequency region may be attributed to release of space charge.

Imaginary part of complex impedance

Figure 2 represents the variation of Imaginary part of complex impedance (Z'') with frequency. The impedance loss spectra have features such as decrease in the height of the peak and shift in peak toward higher frequencies with increasing MWNT concentrations. This confirms better capacitive nature and decrease in resistance of the composites with MWNT loading. The frequencies at which peak occurred are at 98.03, 297.43, 719.95, and 982.862 Hz for 2, 4, 6, and 8 phr of MWNT loading, respectively. This increase in frequency can be explained on the basis of the mechanical and viscoelastic properties of crosslinked and reinforced multiphase polymeric materials. The addition of the filler particles has a significant effect on the dielectric behavior of the sample. Filler particles in the matrix acquires induction charges in presence of the applied external field, polarization effects take place so-called Maxwell–Wagner–Sillar's polarizations. Below the critical concentration of the filler loading, the interparticle distance is large enough so that neighboring local fields apparently do not interact. Thus, dielectric factor in this region increases slowly. But as the filler loading increases, the Maxwell–Wagner–Sillar's effect increases due to reduction in the interaggregate distance giving rise to dielectric properties.

The Z'' data have been fitted to different spectral functions commonly used such as Debye, Cole–Cole, Cole–Davidson, Havriliak–Negami, Frohlich.[17] The best fit was obtained using a Havriliak–Negami function, superimposed with Frohlic function to account the effect of conductivity.

The spectral function $Z''(\omega)$ can be expressed as:

$$Z''(\omega) = Z''(\omega)_{HN} + Z''(\omega)_{Fr} + \frac{\theta\sigma}{\omega}, \quad (1)$$

where $Z''(\omega)_{HN}$ denotes Havriliak–Negami function form and $Z''(\omega)_{Fr}$ denotes Frohlic function, ω denotes the angular frequency, σ is the DC conductivity, and θ is a constant. Havriliak–Negami function is expressed as

$$Z''(\omega)_{HN} = \frac{(Z_s'' - Z_\infty'')\sin\phi\beta}{\left[1 + 2(\omega\tau_{HN})^{1-\alpha}\sin\frac{\pi\alpha}{2} + (\omega\tau_{HN})^{2(1-\alpha)}\right]^{\beta/2}}, \quad (2)$$

$$\text{where } \phi = \arctan\frac{(\omega\tau_{HN})^{(1-\alpha)}\cos\frac{\pi\alpha}{2}}{1 + (\omega\tau_{HN})^{(1-\alpha)}\sin\frac{\pi\alpha}{2}} \quad (3)$$

and Z_s'' and Z_∞'' are the values of Z_s'' at static (at 20 Hz in our case) and at infinite frequency (2 MHz), respectively. The parameters α and β have been found to be 0.186 and 0.587, respectively.

Frohlich function is represented as:

$$Z''(\omega)_{Fr} = \frac{(Z_s'' - Z_\infty'')}{P}\arctan\frac{\sinh P/2}{\cosh\ln(\omega\tau_{Fr})}, \quad (4)$$

where P is a parameter describing the width of the distribution of relaxation times between the two limiting values τ_1 and τ_2 (where $P = \ln(\tau_1/\tau_2)$). τ_{Fr} is the mean relaxation time and is equal to $(\tau_1\tau_2)^{1/2}$. The values of τ_1 calculated at increasing MWNT concentrations of 2, 4, 6, and 8 phr is found to be in the range of 1.02×10^2, 3.36×10^3, 1.326×10^4, and 1.035×10^5 s and τ_2 values as 4.672×10^4, 6.897×10^4, 0.432×10^5, and 4.217×10^5 s, respectively.

Nyquist plots

Figure 3 shows the Nyquist plot [the relationship between imaginary part of impedance (Z'') and real part of impedance (Z')] of butyl rubber composites as a function of increasing MWNT concentrations. It can be observed that increasing filler in the

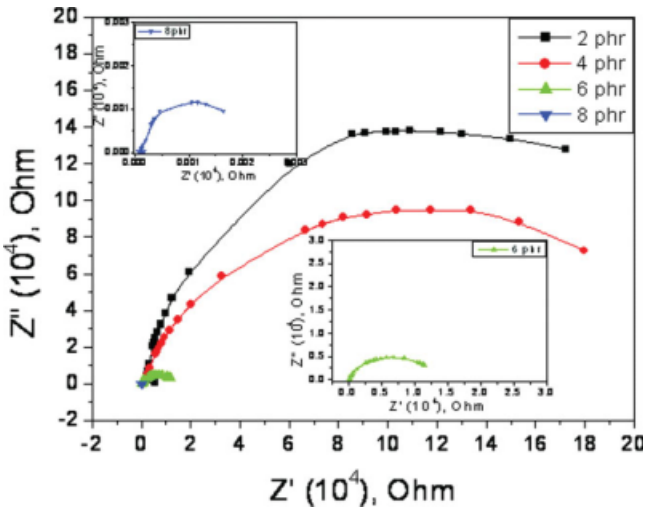

Figure 3 Nyquist plots of butyl elastomer nanocomposites: effect of MWNT loadings. [Color figure can be viewed in the online issue, which is available at www.interscience.wiley.com.]

composite has a sizable effect on the dielectric properties of this system at all frequencies. From the figure, it can also be observed that irrespective of the filler loadings, the plots yield good semicircles indicating the occurrence of polarization with a single relaxation time taking place, i.e., a local mode process dominated. However, at higher filler loadings (6 and 8 phr), the semicircles did not reach the origin and had a small positive intercept on the Z' axis indicating build up of ions at the interphase between the filler and polymer matrix.[18]

Several attempts have been made to interpret the impedance spectroscopy of polymer-filler systems using the resistance–capacitance parallel circuit (RC) model. In a Nyquist plot for a polymer composite system, the real axis represents bulk resistivity (R_B) and the imaginary axis represents ω_{max}, which is given by

$$\omega_{max} = \frac{1}{R_B C_B}, \tag{5}$$

where C_B is the bulk capacitance of the polymer composite. In a Nyquist plot, increase in R_B represents poor conductivity. Figure 3 shows that with increase in MWNT loading, R_B value decreases, or in other words, the composites become more capacitive in nature.

With increasing filler loading, the distance between the aggregates reduces. This gap can be approximated by a parallel plate capacitor with an area (A), separation distance (d), and capacitance (C) ($\varepsilon_0 A/d$), where ε is the dielectric constant of the polymer. Each filler aggregate has a resistance (R_a), the resistance within the aggregate. The impedance in a microcellular composite can be written as

$$Z = R_{as} + \frac{R_{cs}}{1+\omega^2 R_{cs}^2 C_s^2} - j\frac{\omega R_{cs}^2 C_s}{1+\omega^2 R_{cs}^2 C_s^2} \tag{6}$$

The respective imaginary and real parts of impedance can be expresses as:

$$Z' = R_{as} + \frac{R_{cs}}{1+\omega^2 R_{cs}^2 C_s^2} \quad \text{and} \quad Z'' = -\frac{\omega R_{cs}^2 C_s}{1+\omega^2 R_{cs}^2 C_s^2} \tag{7}$$

and the dielectric loss tangent can be expressed as:

$$\tan\delta = \frac{Z''}{Z'} = -\frac{\omega R_{cs}^2 C_s}{R_{as} + R_{cs} + \omega^2 R_{cs}^2 R_{as} C_s^2} \tag{8}$$

From the above equations, the relationship between Z' and Z'' is

$$\left(Z' - \frac{2R_{as} + R_{cs}}{2}\right)^2 + Z_2^2 = \left(\frac{R_{cs}}{2}\right)^2 \tag{9}$$

Therefore a plot of Z'' and Z' will give a half circle, which has the center at $((2R_{as} + R_{cs})/2\,, 0)$ and radius of $R_{cs}/2$.

Wang et al.[19] proposed that because the circular curve of the Z'' vs. Z' occurs only for the parallel resistor circuit, the above analysis can be used to confirm the existence of the capacitor effect. The capacitor effect also confirms that the gap between the nanotubes controls the electron conduction via non-Ohmic contacts between the filler aggregates. The variation in the values of radius and center of the half circle can also be used as a measure of the gaps in between filler aggregates. Using the above equations, the radius and center are calculated and tabulated in Table I. It can be observed that increasing filler loadings the radius reduces and the center shifts to lower values.

It can also be observed that with increasing nanotube concentrations the area under the curve in the Nyquist plot is decreasing. The intensity of this decrease is more pronounced at higher loadings of filler when compared with lower loadings. This can be explained on the basis of "space charge" phenomenon in heterogeneous systems. Filled rubbers are

TABLE I
Radius and Center (for Fig. 3) in MWNT Reinforced Butyl Rubber Nanocomposites

MWNT concentration (phr)	Center (x,0)	Radius
2	3.214×10^5, 0	446
4	9.567×10^4, 0	358
6	4.896×10^4, 0	302
8	8.876×10^3, 0	284

multicomponent systems that have complex molecular, supramolecular, and topological structures, which determine their ultimate properties. These structures are formed during compounding and processing.

The sample preparation of rubber involves operations such as compression, cutting and friction, which cause electrical polarization that leads to the formation of the so-called mechanoelectrets.[20] The lifetime of the polarization charge depends on the polymer nature and the conditions of electret storage and usage (temperature, dielectric characteristics of the polymer, fillers, etc.) This electret state of rubbers has been studied in detail (especially the arising of the electret state during processing) by Pinchuk et al.[21] who proposed that nonconductive rubber when subjected to high-shear stresses could lead to electret formation. These radicals could participate in polarization following several mechanisms: dipolar (directed orientation of molecules), ionic (orientation of quasidipoles created by weakly bonded ions), and bulk (radicals displacement to macrodistance). Increasing filler loadings lead to increased formation of more electrets thereby giving rise to more polarization.

A similar explanation has been given by Levya et al.[22] who reported that the medium frequency relaxation in carbon black reinforced polymers is caused primarily by interfacial polarization, which is due to the buildup of charges on boundaries/interfaces between materials. Application of an external electric field causes polarization of large colloidal particles and creates perturbation in a miniature double layer on each particle, which behaves like a macroion.[23] Under the influence of an external electric field, the counter-ions are redistributed along the surface of filler particles, and hence, a double layer is deformed and polarized, leading to interfacial polarization and the resulting relaxation or dispersion. The magnitude of relaxation of these counter-ions (in the medium frequency region) is much larger than the relaxation due to orientation of dipoles.[24]

Dielectric permittivity

Figure 4 represents the variation in dielectric permittivity as a function of frequency for 2, 4, 6, and 8 phr MWNT reinforced butyl nanocomposites. At fixed frequencies, the dielectric permittivity increases slowly with increasing MWNT concentrations that can be attributed to the dipoles getting less time to orient themselves in the (ever changing) direction of the alternating field. Knite et al[25] explained the variation in dielectric permittivity as a function of frequency in terms of "giant tenso-resistance effect." Irrespective of the fillers used in the polymer matrix, a continuous insulator–conductor transition is observed with gradual increase of the number of

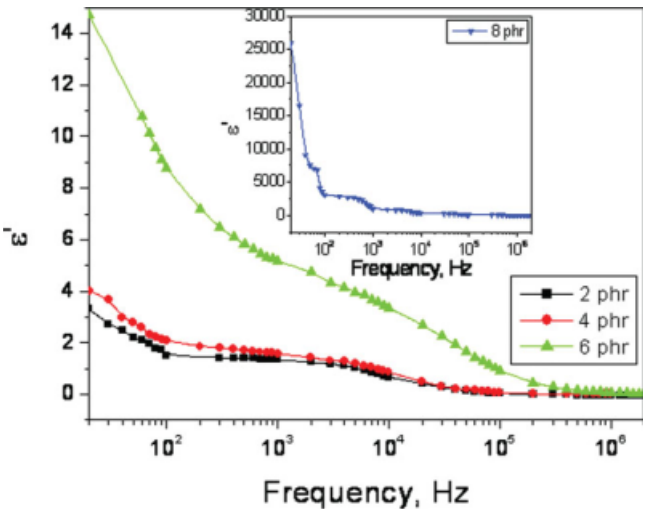

Figure 4 Effect of MWNT loadings on dielectric permittivity (ε′) of butyl elastomer nanocomposites measured as a function of frequency. [Color figure can be viewed in the online issue, which is available at www.interscience.wiley.com.]

randomly dispersed conductor particles in the insulating polymer matrix. The volume concentration (V_C) of conductor particles at which this transition occurs is called as percolation threshold or the critical point.

According to percolation theory, in the vicinity of critical concentration of filler, V_C, the variation in dielectric constant with filler concentration is given by the generalized scaling law:

$$\varepsilon \sim |V - V_C|^{-v} \text{ upon approaching } V_C \qquad (10)$$

In agreement with the general scaling principle of the percolation theory, the relative dielectric permittivity of a two component system (like composite) at low AC frequencies,[23] approaching the percolation threshold from both sides, diverges as ε:

$$\varepsilon \sim |V - V_C|^{-s}, \quad V < V_C, \quad V > V_C \qquad (11)$$

In the vicinity of the percolation threshold, conductivity of the composite changes as:

$$\sigma \sim |V - V_C|^{t} \quad \text{for } V > V_C \qquad (12)$$

$$\text{and} \quad \sigma \sim |V - V_C|^{-q} \quad \text{for } V < V_C \qquad (13)$$

The power indices s, t, and q in the above equations are called as the critical indices of the percolation phase transition.

In the vicinity of percolation, Wilkinson et al.[26] gave some fundamental expressions for dielectric permittivity, ε as a functions of applied frequency f by assuming a random distribution of conductor particles in a well-insulating matrix and modeling

the composite as a network of randomly distributed capacitors.

$$\sigma \sim f^{x} \quad \text{and} \quad \varepsilon \sim f^{-y} \tag{14}$$

and the critical indices x and y are related by the general scaling law: $x + y = 1$.

The scaling law is based on the two theoretical considerations:

a. Polarization of the filler particulates within the insulating matrix (the intercluster polarization theory of Wilkinson and Langer based on classic Maxwell model)
b. Anomalous diffusion of charge carriers within the secondary filler aggregate structures (based on Aharony model of anomalous diffusion)

In case of 3D composites under the assumption of BCC (body centered cubic lattice) structure theoretically the values of x and y are 0.72 and 0.28, respectively, and in FCC (face centered cubic lattice), the values are 0.58 and 0.42. But generally the structure of polymer composites is indeterminate. It depends on wide range of factors like type of filler, its dispersion within the polymer matrix, the interparticle attraction between the filler aggregates, the level of interaction between the polymer matrix and filler particulates(the well-known bound rubber phenomenon), etc. So, the only way of obtaining the values of x and y is by semiempirical methods, in which the observed experimental data are fitted to equations. The values of x and y also provide information regarding the electrodynamic processes within the composite. The value of (x,y) is (0.541,0.457), (0.524,0.476), (0.491,0.506), and (0.441,0.539) for 2, 4, 6, and 8 phr loadings, respectively. These values are nearer to the assumptions of BCC structure.

Cole–Cole plots

Cole–Cole plots for multiwalled nanotube reinforced butyl rubber composites are shown in Figure 5. Irrespective of filler loading at all concentrations of the filler, the usual depressed semicircular can be observed, which clearly indicates the presence of a capacitive element. The large change observed on the arc radius in the Cole–Cole plot of the composite clearly indicates that there is a charge transfer between the nanotubes and the polymer. This result accompanied by a shift to a higher frequency of the Z″ curve peak suggests a significant alteration of chain conformation due to nanotube interaction.[27] McLachlan et al. correlated the shape of Cole–Cole plots with the homogeneity of MWNT dispersion in the polymer matrix. Irrespective of MWNT concentrations, smooth arcs are observed with no humps

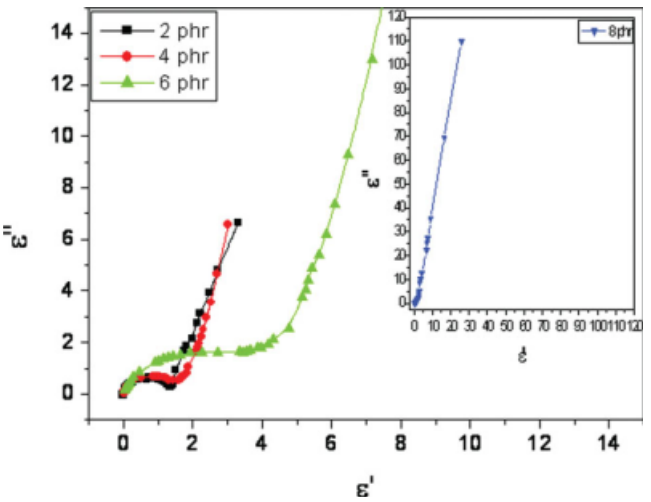

Figure 5 Cole–Cole plots of MWNT reinforced butyl elastomer nanocomposites: effect of MWNT loadings. [Color figure can be viewed in the online issue, which is available at www.interscience.wiley.com.]

indicating good dispersion of MWNT in the polymer matrix.[28] Representative SEM micrographs shown in Figure 6 taken at increasing MWNT concentrations shows excellent distribution of MWNT in the polymer matrix.

Raman spectra as a tool to study charge transfer mechanism in polymer-nanotubes composites has been reported by Wise et al.[29] Representative Raman spectra of MWNT powder and 8 phr MWNT reinforced IIR composite is shown in Figure 7. From the figure it can be observed that in all the bands (D, G, and D′ bands) a shift in peak location of polymer composites can be observed. This result is consistent with the reports of Wise et al[29] who reported that if nanotubes were to lose charge to the polymer matrix, one would expect an upward shift in G band, conversely if charge is gained from the polymer matrix a downward shift can be expected. On the basis of this theory, our results indicate that MWNTs gain charge from the polymer matrix.

Complex dielectric modulus

Electrical response of the samples can be analyzed in terms of complex dielectric modulus formalism, which provides an alternative approach based on polarization analysis. Complex impedance spectrum gives more emphasis to elements with the largest resistance, whereas complex dielectric modulus plots highlight with smallest capacitance. Using the complex dielectric formalism, the inhomogeneous nature can be probed into bulk and grain boundary effects, which may not be detected/distinguished from complex impedance plots. The other advantage of the dielectric modulus formalism is that the electrode effect can be suppressed. The complex dielectric

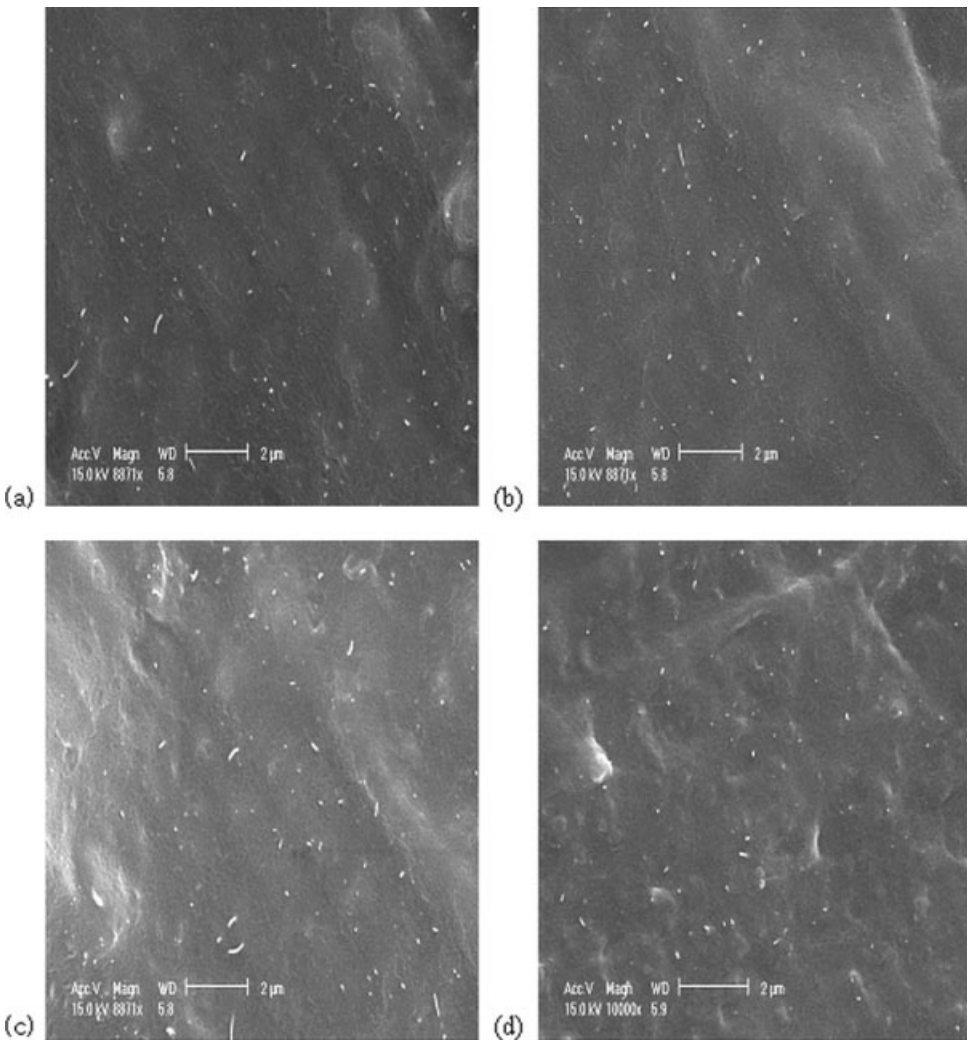

Figure 6 State of dispersion of MWNT in butyl elastomer, (a) 2 phr MWNT, (b) 4 phr MWNT, (c) 6 phr MWNT, and (d) 8 phr MWNT.

modulus (M^*) have been calculated from the dielectric parameters suvh as dielectric permittivity (ε') and dielectric loss (ε'') using the following relations:

$$M^* = \frac{1}{\varepsilon^*} = \frac{1}{\varepsilon' - i\varepsilon''} = \frac{\varepsilon'}{(\varepsilon')^2 + (\varepsilon'')^2} + i\frac{\varepsilon''}{(\varepsilon')^2 + (\varepsilon'')^2} = M' + iM'' \quad (15)$$

where M' is real part and M'' is imaginary part of complex electric modulus and $i = \sqrt{-1}$. Based on the above equation, the dielectric data can be represented as $M'(\omega)$ and $M''(\omega)$ in stead of $\varepsilon'(\omega)$ and $\varepsilon''(\omega)$, respectively, where ω is angular frequency, i.e., $2\pi f$ and f is measured frequency in Hz.

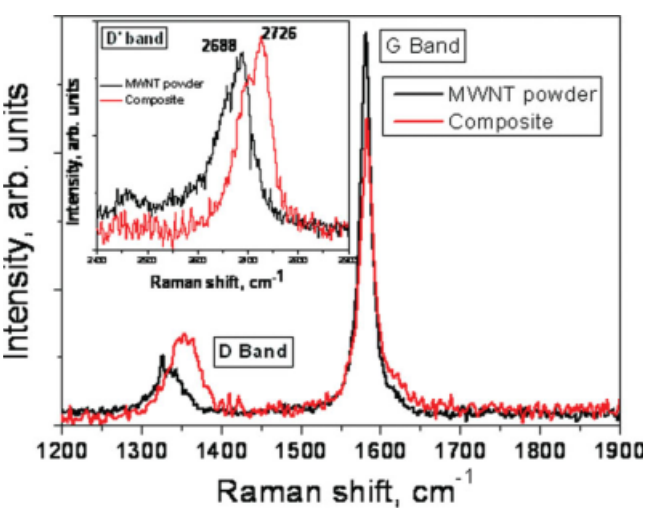

Figure 7 High-frequency Raman spectra of MWNT and IIR/MWNT composite, insert in figure represents Raman shift in D′ band. [Color figure can be viewed in the online issue, which is available at www.interscience.wiley.com.]

Real part of complex dielectric modulus

Figure 8 shows frequency-dependent real part of complex dielectric modulus (M'). A gradual increase of real part of complex dielectric modulus with

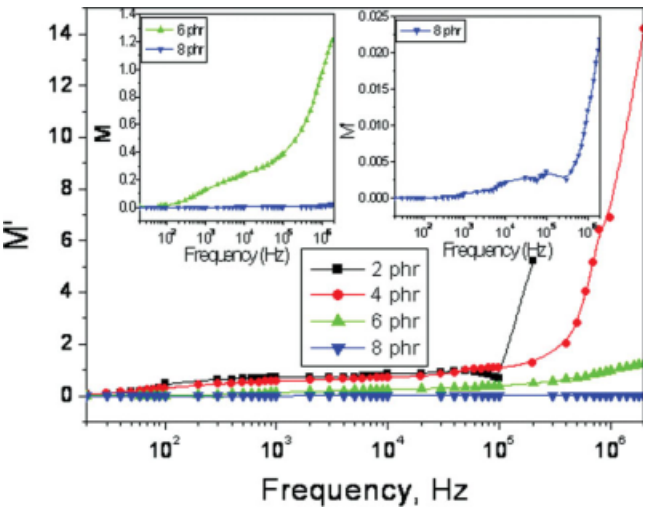

Figure 8 Effect of MWNT loadings on real part of complex modulus (M') of butyl elastomer nanocomposites measured as a function of frequency. [Color figure can be viewed in the online issue, which is available at www.interscience.wiley.com.]

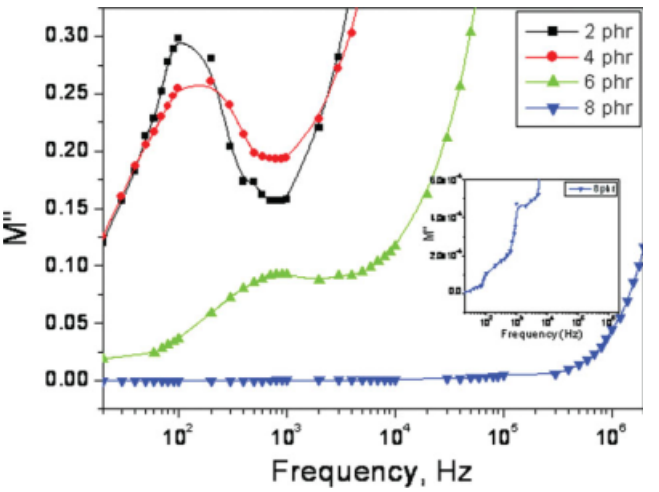

Figure 9 Effect of MWNT loadings on imaginary part of complex modulus (M'') of butyl elastomer nanocomposites measured as a function of frequency. [Color figure can be viewed in the online issue, which is available at www.interscience.wiley.com.]

frequency is observed for all MWNT loadings. It is characterized by a very low value M' in the low-frequency region. A continuous dispersion with increase in frequency has a tendency to saturate at a maximum asymptotic value in the high-frequency region for all MWNT loading. Such observations may possibly be related to a lack of restoring force governing the mobility of charge carriers under the action of an induced electric field. This behavior supports long-range mobility of charge carriers. Further, a sigmoidal increase in the value of M' with increasing frequency approaching ultimately maximum value may be attributed to the conduction phenomenon due to short-range mobility of charge carriers.

Imaginary part of complex dielectric modulus

Figure 9 shows the variation of the imaginary (M'') part of the electric modulus with frequency at different MWNT loadings. In the accessible frequency range, the spectrum at each MWNT loading exhibited one relaxation peak. The peaks shift systematically toward higher frequencies with increase in MWNT loading. For 2, 4, 6, and 8 phr MWNT loading, peak is observed at 100, 200, 700, and 1000 Hz, respectively. The broadening of the peak indicates the spread of relaxation time with different (mean) time constants, and hence a non-Debye type of relaxation in the materials is observed. This is very much consistent with the impedance data. The nature of the processes is further explored using the Argand diagram (complex plane representation) for dielectric modulus as shown in Figure 10 for all MWNT loadings.

Argand diagram

Figure 10 shows the relationship between real part (M') and imaginary part (M'') of dielectric modulus so-called Argand diagram for all MWNT loadings. A semicircular trend (a requirement for non-Debye model) followed by a linear increase is observed for all MWNT loadings. It is also observed that with increase in MWNT loading the size of the semicircular loop decreases, which confirms better conduction. So, the presence of a non-Debye type of relaxations has been confirmed by complex dielectric modulus analysis.

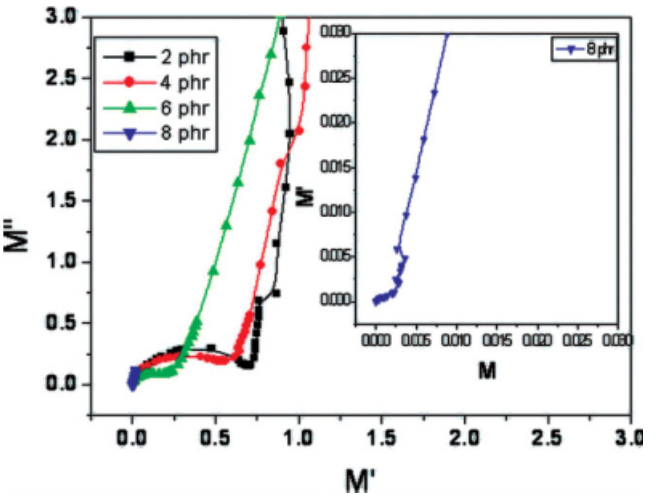

Figure 10 Argand diagram of butyl elastomer nanocomposites: effect of MWNT loadings. [Color figure can be viewed in the online issue, which is available at www.interscience.wiley.com.]

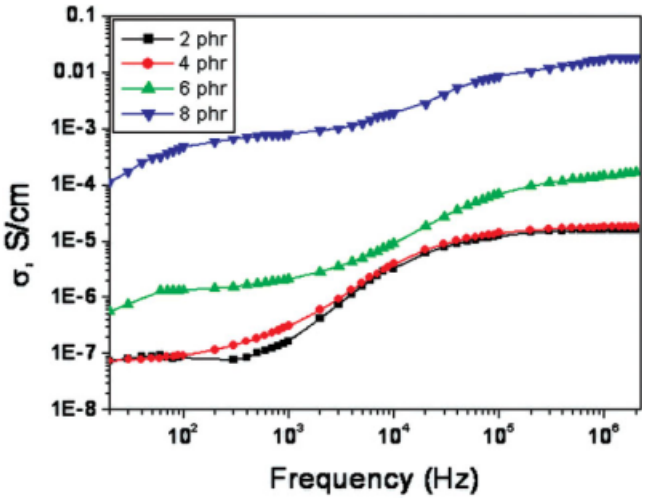

Figure 11 Effect of MWNT loadings on electrical conductivity (σ) of Butyl elastomer nanocomposites measured as a function of frequency. [Color figure can be viewed in the online issue, which is available at www.interscience.wiley.com.]

Electrical conductivity

Figure 11 shows the variation of electrical conductivity with frequency at increasing MWNT concentrations in butyl rubber. At any given frequency, tremendous increase in conductivity with increasing filler concentration can be observed. Figure shows the variation of conductivity with frequency for IIR/MWNT nanocomposites at increasing MWNT concentrations. From the figure three different regions: frequency independent region (Region 1), exponential growth with increasing frequency (Region 2), and finally a plateau region (Region 3). The shift from Region 1 to Region 2 depends on the MWNT concentration and is 296.5, 105.1, 57.87, and 20 Hz in 2, 4, 6, and 8 phr, respectively. In fact in 8 phr composites, Region 1 is completely absent.

It is widely believed that electrical properties of reinforced polymers depend primarily on the way the filler particles are distributed through the polymer matrix also called the mesostructure. At low levels of filler loading, the conductivity of the composite is slightly higher than that of the base polymer, because the filler particles are isolated from each other by the insulating polymer matrix. When concentration of MWNT is low, the conductivity between the grains of filler is expected to be primarily via hopping and tunneling mechanisms. In this mode of conduction, the electron transport may be coupled strongly with the molecular and ionic processes in the polymer matrix. Usually, hopping transport between localized sites is the main reason for the frequency dependence of conductivity in polymer composites. The dispersion of filler is heterogeneous, localized, and disordered. This disorder results in a wide distribution of hopping rates, giving a strong dispersion of the AC conductivity.[30]

Considering the RC parallel circuit model, with increase in MWNT loading, the filler particles get more tightly packed and more intensely pressed against each other. This leads to a net reduction in the internal contact resistance (R_C) and therefore, the net resistance ($R_C + R_A$) decreases with increase in the filler loading level. Here, R_A indicates resistance within the conducting dispersed MWNT, and R_C is the contact resistance. With increasing MWNT concentration, the gaps between conducting particle agglomerates become smaller or negligible (at percolation limit) and the net resistance becomes practically equal to R_A. This would usually happen for high enough loading using conducting filler. Hence, conductivity increases with filler loading.

In most of the polymer composites, a power law dependence of conductivity (σ) is observed with the variation in frequency (ω), which is represented mathematically by:

$$\sigma_{a.c.}(\omega) \propto \omega^s \quad \text{or} \quad \sigma_{a.c.}(\omega) = A\omega^s, \tag{16}$$

where A is constant, and the value of the exponential parameter, s ranging from $0 < s \leq 1$, but mostly the value of $s \approx 1$. The frequency dependence of conductivity usually a small d.c. conductivity to a high-localized one (at increasing frequencies) and is attributed to the polarization of the increasingly small conducting units. In disordered materials, electron transport relevant mechanisms are electron localization with associated hopping and fractal topology.[31]

According to Jonscher[32] the electrical conductivity of many disordered solids (including polymer composites) was found to be sum of d.c. conductivity (independent of frequency) and a.c. conductivity (strongly frequency dependent). It was noted that the overall frequency dependence of σ (so-called "universal dynamic response" of electron conductivity) could be approximated by the following simple relation:

$$\sigma = \sigma_{dc} + \sigma_{a.c.} \quad \text{or} \quad \sigma = \sigma_{dc} + A\omega^s, \tag{17}$$

where $\omega = 2\pi f$ is the angular frequency, A is constant, and s is exponential parameter. For a polymer composite containing moderate concentration of filler, $s \approx 0.5$–0.6, and both σ and A follow strong dependencies on a variety of factors including the filler loading and temperature. The values of A and s depend on MWNT loading of butyl composites and is shown in Table II. It can be observed that the value of s increases on increasing volume fraction of filler; however, the increase in the value of A is marginal.

TABLE II
Variation in Parameters *A* and *s* on Increasing MWNT Concentrations in Butyl Rubber Nanocomposites

MWNT concentration (phr)	*s*	*A*
2	0.245	78.254
4	0.314	79.932
6	0.478	81.451
8	0.569	83.247

Percolation

The variation of electrical conductivity and dielectric permittivity with MWNT loadings in butyl nanocomposites is shown in Figure 12(a,b), respectively. The electrical conductivity and dielectric permittivity of a composite is generally characterized by its dependence on volume fraction of filler. It can be observed at all frequencies (10^2, 10^3, 10^4, 10^5,and 10^6 *Hz*), above 6 phr MWNT loading there is an abrupt increase in parameter implying the occurrence of a percolation limit. As the concentration of MWNT in the composite is increased, the filler particles begin to contact each other and a continuous path is formed through the volume of the sample for electrons to travel. The formation of this conductive network is based on the principles of percolation theory. Beyond a critical concentration of the filler, known as the percolation threshold, an increase of the composite conductivity of several orders of magnitude is observed.

The relationship between MWNT content and conductivity can be described by the following power law equation:

$$\sigma = \sigma_0 \left| 1 - \frac{\phi}{\phi_c} \right|^{-x}, \tag{18}$$

where σ_0 is the conductivity of butyl matrix, ϕ_c is the percolation threshold, and x is a critical exponent. As can be observed from Figure 12(a), the experimental values agree reasonably with above equation when $\phi_c = 1.83\%$ and $x = 1.21$.

The dielectric constant of butyl rubber/MWNT vs. MWNT volume fraction [Fig. 12(b)] shows a similar percolation phenomenon is observed. The dependence of dielectric constant of IIR/MWNT nanocomposites on MWNT concentration can also be expressed by the following power law relations:

$$\varepsilon = \varepsilon_0 \left| 1 - \frac{\phi}{\phi_c} \right|^{-s'}, \tag{19}$$

where ε_0 is the dielectric constant of butyl matrix, ϕ_c is the percolation threshold, and s' is the critical exponent. From figure, the experimental data are in good agreement with eq. (21) with $\phi_c = 1.83\%$ and $s = 0.96$.

The percolation concentration of polymer composites containing conductive fillers of large aspect ratios can also be satisfactorily predicted by using the excluded volume concept proposed by Balberg et al.[33,34]

In three-dimensional systems, the critical volume fraction ϕ_c of fillers can be related to the total exclude volume of filler $\langle V_{ex} \rangle$ by the following expression given by Balberg:

$$\phi_c = 1 - \exp\left(-\frac{\langle V_{ex} V \rangle}{\langle V_e \rangle} \right) = 1 - \exp(-N_c V), \tag{20}$$

where $\langle V_{ex} \rangle$ is the product of the critical number density N_c and the excluded volume $\langle V_{ex} \rangle$ of fillers, V is the real volume of individual MWNT.

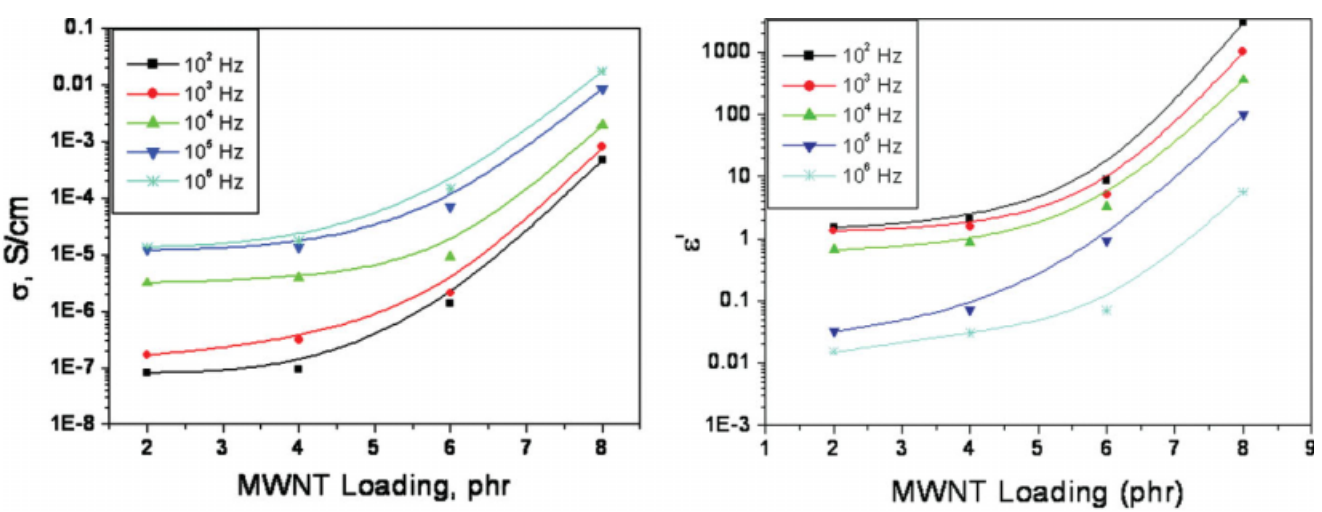

Figure 12 (a) Effect of MWNT loading on electrical conductivity of butyl elastomer nanocomposites at different frequencies. (b) Effect of MWNT loading on dielectric permittivity of butyl elastomer nanocomposites at different frequencies. [Color figure can be viewed in the online issue, which is available at www.interscience.wiley.com.]

For anisotropic fillers with the critical volume fraction ϕ_c of a capped cylinder of length L and diameter W by the following expression given by Celzard et. al.[35]

$$\phi_c = 1 - \exp\left(-\frac{\langle V_{ex}\rangle\left[\left(\frac{\pi}{4}\right)W^2L + \left(\frac{\pi}{6}\right)W^3\right]}{\left(\frac{4\pi}{3}\right)W^3 + 2\pi W^2L + \left(\frac{\pi}{4}\right)WL^2}\right) \quad (21)$$

The upper and lower bounds of $\langle V_{ex}\rangle$ is 1.4 for thin cylindrical particles (if good dispersion of filler) and 2.8 for spherical fillers(aggregated).

$$1 - \exp\left(-\frac{1.4V}{\langle V_e\rangle}\right) \leq \phi_c \leq 1 - \exp\left(-\frac{2.8V}{\langle V_e\rangle}\right) \quad (22)$$

Under the assumption that the length and diameter of MWNTs lie in the range diameter range: 10–15 nm; length range: 2–3 μm[36] the critical concentrations of the above double inequality is determined to be $0.16\% \leq \phi_c \leq 3.6\%$. Comparing with the predicted value, the experimentally determined value is 0.28%, which is nearer to the assumption of thin cylindrical particles which again confirms that the dispersion of nanotubes in the polymer matrix is good.

CONCLUSIONS

The dielectric relaxation of multiwalled carbon nanotube reinforced butyl elastomer composites has been studied as function of increasing filler loading in the frequency range of 20 Hz–2 MHz. Irrespective of the amount of filler in the composite a decrease in real part of impedance with increasing frequencies has been observed, which was indicative of the capacitance nature of the composites. The variation of complex part of impedance with applied frequency showed a distinct peak, the occurrence of which was dependent on the amount of filler in the composite. Increasing filler loadings also lead to increase in nonsemicircle nature of the Nyquist plots. This phenomenon was analyzed on the basis of resistance–capacitance circuit. The percolation limit of the filler in the composite has been studied by electrical conductivity measurements. It has been observed that the percolation limit was occurring in between 6 and 8 phr loading.

References

1. Kraus, G. Reinforcement in Elastomers; Wiley-Interscience: New York, 1965.
2. Sridhar, V.; Chaudhary, R. N. P.; Tripathy, D. K. J Appl Polym Sci 2006, 100, 3161.
3. Xu, D.; Sridhar, V.; Pham, T. T.; Kim, J. K. E-Polymers 2008, 23, 1.
4. Pham, T. T.; Sridhar, V.; Kim, J. K. Polym Comp 2009, 30, 121.
5. Bokobza, L.; Kolodzeij, M. Polym Int 2006, 55, 1090.
6. Bokobza, L. Polymer 2007, 48, 4907.
7. Wang, S. Characterization and Analysis of Electrical Conductivity Properties of Nanotube Composites, MS Thesis, Department of Industrial Engineering, FAMU-FSU College of Engineering, 2005.
8. Jeroen, W. G. W.; Liesbeth, C. V.; Andrew, G. R.; Richard, E. S. Nature 1998, 391, 59.
9. Zhao, Q.; Tannenbaum, R.; Jacob, K. I. Carbon 2006, 44, 1740.
10. Shanmugharaj, A. M.; Bae, J. H.; Lee, K. Y.; Noh, W. H.; Lee, S. H.; Ryu, S. H. Comp Sci Tech 2007, 67, 1813.
11. Fakhrul-Razi, A.; Atieh, M. A.; Girun, N.; Chuah, T. G.; El-Sadiq, M.; Biak, D. R. A. Comp Struc 2006, 75, 496.
12. Sui, G.; Zhong, W.; Yang, X.; Zhao, S. Macro Mat Eng 2007, 292, 1020.
13. Bokobza, L.; Diop, A. L.; Fournier, V.; Minne, J.-P.; Bruneel, J. L. Macro Symp 2005, 230, 87.
14. Chen, X. H.; Song, H. H. N Carb Mater 2004, 19, 214.
15. Park, I. S.; Kim, K. J.; Nam, J. D.; Lee, J.; Yim, W. Polym Eng Sci 2007, 47, 1396.
16. El-Tantawy, F.; Bakry, A.; El-Gohary, A. R. Polym Int 2000, 49, 1670.
17. Mc-Crum, N. G.; Read, B. E.Williams, G. Anelastic and Dielectric Effects in Polymeric Solids, Dover edition; Dover Inc.: New York, 1991.
18. Jawad, S. A.; Alnajjar, A. Polym Int 1997, 44, 208.
19. Wang, Y. J.; Pan, Y.; Zhang, X. W.; Tan, K. J App Polym Sci 2005, 98, 1344.
20. Kestelman, V.; Pinchuk, L.; Goldade, V. Electrets in Engineering: Fundamentals and Applications; Kluwer Academic Publishers: Boston, MA, 2000
21. Pinchuk, L.; Jurkowski, B.; Jurkowoska, B.; Kravtov, A.; Goldade, V. Eur Polym J 2001, 37, 2239.
22. Leyva, M. E.; Barra, G. M. O.; Moreira, A. C. F.; Soares, B. G.; Khastgir, D. J Polym Sci Part B: Polym Phys 2003, 41, 2983.
23. Grimnes, S.; Martinsen, O. G. Bioimpedance and Bioelectricity Basics, 1st ed.; Academic Press: New York, 2000.
24. Bearchell, C. A.; Edgar, J. A.; Heyes, D. M.; Taylor, S. E. J Colloid Interface Sci 1999, 210, 231.
25. Knite, M.; Teteris, V.; Kiploka, A.; Klemenoks, I. Adv Eng Mater 2004, 6, 742.
26. Wilkinson, D.; Langer, J. S.; Sen, P. N. Phys Rev B 1983, 28, 1081.
27. Valentini, L.; Amentano, I.; Biagotti, J.; Frulloni, E.; Kenny, J. M.; Santucci, S. Diamond Relat Mater 2003, 12, 1601.
28. McLachlan, D. S.; Chiteme, C.; Park, C.; Wise, K. E.; Lowther, S. E.; Lillehei, P. T.; Siochi, E. J.; Harrison, J. S. J Polym Sci Part B: Polym Phys 2005, 43, 3273.
29. Wise, K. E.; Park, C.; Siochi, E. J.; Harrison, J. S. Chem Phys Lett 2004, 391, 207.
30. Bottger, H.; Bryskin, V. V. Hopping conduction in solids; Akademie-Verlag: Berlin, 1985.
31. Ghosh, P.; Chakrabarti, A. Eur Polym J 2000, 36, 1043.
32. Jonscher, A. K. Nature 1979, 267, 673.
33. Balberg, I.; Anderson, C. H.; Alexander, S.; Wagner, N. Phys Rev B 1984, 30, 3933.
34. Balberg, I. Phys Rev B 1986, 33, 3618.
35. Celzard, A.; McRae, E.; Deleuze, C.; Dufort, M.; Furdin, G.; Mareche, J. F. Phys Rev B 1996, 53, 6209.
36. Cooper, C. A.; Ravich, D.; Lips, D.; Mayer, J.; Wagner, H. D. Comp Sci Tech 2002, 62, 1105.